Dual gratings for enhanced light trapping in thin-film solar cells by a layer-transfer technique

Christian S. Schuster,[1,*] Piotr Kowalczewski,[2] Emiliano R. Martins,[3] Maddalena Patrini,[2] Mark G. Scullion,[1] Marco Liscidini,[2] Liam Lewis,[4] Christopher Reardon,[1] Lucio C. Andreani,[2] and Thomas F. Krauss[1]

[1]*Department of Physics, University of York, York, YO10 5DD, UK*
[2]*Department of Physics, University of Pavia, Via Bassi 6, 27100 Pavia, Italy*
[3]*School of Physics and Astronomy, SUPA, University of St Andrews, St. Andrews, KY16 9SS, UK*
[4]*Photonics Device Dynamics Group, Tyndall National Institute, Lee Maltings, Cork, Ireland*
[*]*christian.schuster@york.ac.uk*

Abstract: Thin film solar cells benefit significantly from the enhanced light trapping offered by photonic nanostructures. The thin film is typically patterned on one side only due to technological constraints. The ability to independently pattern both sides of the thin film increases the degrees of freedom available to the designer, as different functions can be combined, such as the reduction of surface reflection and the excitation of quasiguided modes for enhanced light absorption. Here, we demonstrate a technique based on simple layer transfer that allows us to independently pattern both sides of the thin film leading to enhanced light trapping. We used a 400 nm thin film of amorphous hydrogenated silicon and two simple 2D gratings for this proof-of-principle demonstration. Since the technique imposes no restrictions on the design parameters, any type of structure can be made.

OCIS codes: (040.5350) Photovoltaic; (050.1950) Diffraction gratings; (050.5298) Photonic crystals; (310.6628) Subwavelength structures, nanostructures; (350.4238) Nanophotonics and photonic crystals; (350.6050) Solar energy.

References and links

1. M. A. Green, J. Zhao, A. Wang, and S. R. Wenham, "Progress and outlook for high-efficiency crystalline silicon solar cells," Sol. Energy Mater. Sol. Cells **65**(1–4), 9–16 (2001).
2. C. H. Henry, "Limiting efficiencies of ideal single and multiple energy gap terrestrial solar cells," J. Appl. Phys. **51**(8), 4494–4500 (1980).
3. A. Bozzola, M. Liscidini, and L. Andreani, "Photonic light-trapping versus Lambertian limits in thin film silicon solar cells with 1D and 2D periodic patterns," Opt. Express **20** (S2 Suppl 2), A224–A244 (2012).
4. P. Kowalczewski, M. Liscidini, and L. C. Andreani, "Engineering Gaussian disorder at rough interfaces for light trapping in thin-film solar cells," Opt. Lett. **37**(23), 4868–4870 (2012).
5. H. A. Atwater and A. Polman, "Plasmonics for improved photovoltaic devices," Nat. Mater. **9**(3), 205–213 (2010).
6. L. Zhao, Y. H. Zuo, C. L. Zhou, H. L. Li, H. W. Diao, and W. J. Wang, "A highly efficient light-trapping structure for thin-film silicon solar cells," Sol. Energy **84**(1), 110–115 (2010).
7. E. R. Martins, J. Li, Y. Liu, J. Zhou, and T. F. Krauss, "Engineering gratings for light trapping in photovoltaics: the supercell concept," Phys. Rev. B **86**(4), 041404 (2012).
8. E. Yablonovitch, "Inhibited spontaneous emission in solid-state physics and electronics," Phys. Rev. Lett. **58**(20), 2059–2062 (1987).
9. K. R. Catchpole and M. A. Green, "A conceptual model of light coupling by pillar diffraction gratings," J. Appl. Phys. **101**(6), 063105 (2007).
10. P. Sheng, A. N. Bloch, and R. S. Stepleman, "Wavelength-selective absorption enhancement in thin-film solar cells," Appl. Phys. Lett. **43**(6), 579 (1983).
11. R. Dewan, M. Marinkovic, R. Noriega, S. Phadke, A. Salleo, and D. Knipp, "Light trapping in thin-film silicon solar cells with submicron surface texture," Opt. Express **17**(25), 23058–23065 (2009).
12. D. Madzharov, R. Dewan, and D. Knipp, "Influence of front and back grating on light trapping in microcrystalline thin-film silicon solar cells," Opt. Express **19**(S2 Suppl 2), A95–A107 (2011).

#184707 - $15.00 USD Received 5 Feb 2013; revised 8 Mar 2013; accepted 11 Mar 2013; published 22 Apr 2013

13. M. A. Tsai, H. W. Han, Y. L. Tsai, P. C. Tseng, P. Yu, H. C. Kuo, C. H. Shen, J. M. Shieh, and S. H. Lin, "Embedded biomimetic nanostructures for enhanced optical absorption in thin-film solar cells," Opt. Express **19**(S4 Suppl 4), A757–A762 (2011).
14. K. X. Wang, Z. Yu, V. Liu, Y. Cui, and S. Fan, "Absorption enhancement in ultrathin crystalline silicon solar cells with antireflection and light-trapping nanocone gratings," Nano Lett. **12**(3), 1616–1619 (2012).
15. A. Abass, K. Q. Le, A. Alù, M. Burgelman, and B. Maes, "Dual-interface gratings for broadband absorption enhancement in thin-film solar cells," Phys. Rev. B **85**(11), 115449 (2012).
16. X. Meng, E. Drouard, G. Gomard, R. Peretti, A. Fave, and C. Seassal, "Combined front and back diffraction gratings for broad band light trapping in thin film solar cell," Opt. Express **20**(S5 Suppl 5), A560–A571 (2012).
17. Z. Yu, A. Raman, and S. Fan, "Fundamental limit of light trapping in grating structures," Opt. Express **18**(S3 Suppl 3), A366–A380 (2010).
18. H. Stiebig, N. Senoussaoui, C. Zahren, C. Haase, and J. Müller, "Silicon thin-film solar cells with rectangular-shaped grating couplers," Prog. Photovolt. Res. Appl. **14**(1), 13–24 (2006).
19. C. Haase and H. Stiebig, "Optical properties of thin-film silicon solar cells with grating couplers," Prog. Photovolt. Res. Appl. **14**(7), 629–641 (2006).
20. O. Isabella, A. Campa, M. Heijna, W. Soppe, A. Van Erven, R. Franken, H. Borg, and M. Zeman, "Light scattering properties of surface-textured substrates for thin-film solar cells," in *Proceedings of the 23rd EUPVSEC*, 476–481 (2008).
21. C. Hsu, C. Battaglia, C. Pahud, Z. Ruan, F. Haug, S. Fan, C. Ballif, and Y. Cui, "High-efficiency amorphous silicon solar cell on a periodic nanocone back reflector," Adv. Energy Mater. **2**(6), 628–633 (2012).
22. C. Battaglia, C. M. Hsu, K. Söderström, J. Escarré, F. J. Haug, M. Charrière, M. Boccard, M. Despeisse, D. T. L. Alexander, M. Cantoni, Y. Cui, and C. Ballif, "Light trapping in solar cells: can periodic beat random?" ACS Nano **6**(3), 2790–2797 (2012).
23. G. Gomard, X. Meng, E. Drouard, K. E. Hajjam, E. Gerelli, R. Peretti, A. Fave, R. Orobtchouk, M. Lemiti, and C. Seassal, "Light harvesting by planar photonic crystals in solar cells: the case of amorphous silicon," J. Opt. **14**(2), 024011 (2012).
24. M. Agio and L. Andreani, "Complete photonic band gap in a two-dimensional chessboard lattice," Phys. Rev. B **61**(23), 15519–15522 (2000).
25. M. Liscidini, D. Gerace, L. Andreani, and J. E. Sipe, "Scattering-matrix analysis of periodically patterned multilayers with asymmetric unit cells and birefringent media," Phys. Rev. B **77**(3), 035324 (2008).
26. C. Heine and R. H. Morf, "Submicrometer gratings for solar energy applications," Appl. Opt. **34**(14), 2476–2482 (1995).
27. G. F. Feng, M. Katiyar, J. R. Abelson, and N. Maley, "Dielectric functions and electronic band states of a-Si and a-Si:H," Phys. Rev. B Condens. Matter **45**(16), 9103–9107 (1992).

1. Introduction

Thin film solar cells are an emerging technology with the potential to deliver low-cost and efficient photovoltaic solar energy generation [1]. Once the absorbing layers become very thin (i.e. comparable to the wavelength of light), light trapping schemes are required to compensate for the otherwise poor light absorption. The theoretical efficiency of such schemes is a function of both the material dependent energy bandgap [2] and the absorber thickness [3]. Once the material and its thickness have been chosen, the light trapping nanostructure is designed to couple the incident light into the discrete modes of the thin absorbing layer over an extended wavelength and angular range.

Structures for light trapping vary from engineered rough interfaces [4], metal particles [5] to photonic crystals [6] and other types of diffraction gratings [7]; however, the experimentally demonstrated approaches are still well below the theoretical limit, usually taken as the Lambertian limit [8]. The design and realization of an optimal light trapping structure are therefore key aspects of today's research. In particular, diffractive structures can be used either as front anti-reflection layers [9] or as back reflectors [10]. Some groups have already analyzed the case of implementing both structures at the same time [11–16], which increases the degrees of freedom available for light trapping design and promises thin film cells that approach the Lambertian limit more closely [17]. So far, the theoretical designs have been limited to supercell-type calculations where the period on one side was the multiple of that on the other, and experimental structures were limited to those with the same period on both sides, i.e. deposited by conformal growth techniques [18–22].

Here, we outline a fast and simple method for realizing a double-sided grating structure where both gratings can be fabricated independently. As a proof of concept, we demonstrate the fabrication of two simple 2D gratings etched into the top and bottom of a 400 nm thin film of hydrogenated amorphous silicon (a-Si:H). The fabrication method allows us to study

#184707 - $15.00 USD Received 5 Feb 2013; revised 8 Mar 2013; accepted 11 Mar 2013; published 22 Apr 2013

the absorption enhancement of a double-sided grating structure without any restrictions on the design parameters.

2. Design and fabrication

We use a 2D square lattice of holes for our proof-of-principle demonstration. Such 2D square lattices have been studied widely and are well characterized [3]. For a 400 nm thick a:Si layer, 2D gratings with a periodicity of 300-600 nm have been shown to be effective, and we chose a period of 300 nm as a representative example on both sides; using the same period on both sides also makes the computational comparison easier.

The fabricated top and bottom gratings are shown in Figs. 1(a) and 1(b), respectively. We varied the fill-factor of the two gratings in order to facilitate a clear identification of their respective effects; therefore, the bottom grating appears as a well-defined 2D lattice of holes in Fig. 1, while the top grating resembles a square lattice of star-like columns in air. We note that this particular design was chosen for its simplicity, and we believe that further improvements can be implemented, e.g. by using two different periods, which will be the focus of future work.

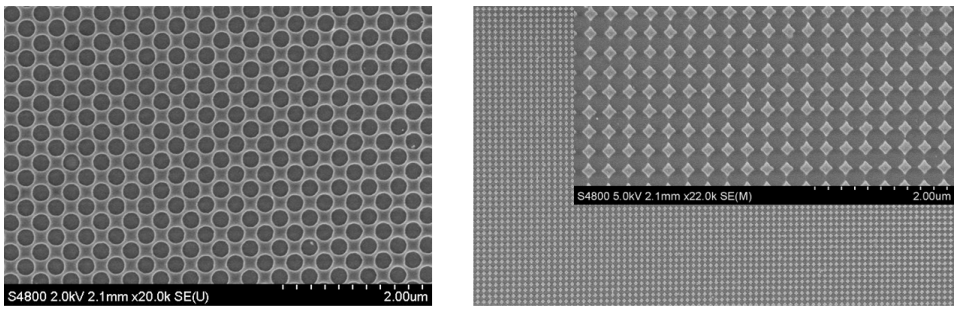

Fig. 1. Scanning electron microscopy (SEM) images of the 2D dual interface grating (a) The bottom grating is a photonic lattice of SiO_2 holes in a-Si:H with a period of 300 nm. The measured hole diameter and nominal etching depth are 240 nm and 60 nm, respectively. (b) The hole diameter of the top grating is set to 300 nm, which is also the lattice period, such that the air holes touch each other. The top grating therefore resembles a chessboard lattice [24], i.e. star-like columns of a-Si:H in air. The nominal etch depth is 80 nm.

The layer transfer technique described next is the core of the process. It is based on using Norland Optical Adhesive (NOA61) which is highly resistant to most chemicals and high temperatures up to 125°C. First, a layer of a-Si:H is deposited by plasma enhanced chemical vapor deposition (PECVD) onto a glass carrier and patterned using conventional lithographic and dry etching techniques (here, we use e-beam lithography). A second carrier is then prepared and both carriers are cleaned in acetone and IPA (five minutes each) and dehydrated on a hot place at 200°C for ten minutes. The surfaces are then plasma ashed in oxygen to guarantee good bonding to the glue and the samples are left on a hotplate at 100°C. NOA61 is then drop-cast onto the carrier with the a-Si:H film and spun at 1800 rpm for 30 seconds. The heat treatment of NOA61 improves the homogeneity of the thin film and avoids the formation of cracks. The second carrier is then placed onto the first one (without any cooling phase) and cured in UV light, with an exposure dose of 700 mJ/cm^2, for 30 minutes. Following exposure, the two carriers can be prised apart. The technique relies on the fact that the a-Si:H film adheres more strongly to the cured NOA61 than to the original glass carrier. We thus were able to transfer films up to 4 cm^2 surface area.

The transferred film is then patterned for a second time. Lithography can proceed as usual because of the resilience of the NOA61 film, including baking of the resist film at 180°C, but warm chemical solutions such as the standard resist remover 1165 above 30°C should be avoided, as these do affect the glue. For this reason, we remove the ZEP mask by an oxygen plasma rather than by dissolving it in 1165. Figure 2(a) shows a top view image of the

#184707 - $15.00 USD Received 5 Feb 2013; revised 8 Mar 2013; accepted 11 Mar 2013; published 22 Apr 2013

sample after the fabrication process, while Fig. 2(b) gives a cross-sectional scheme of the obtained structure.

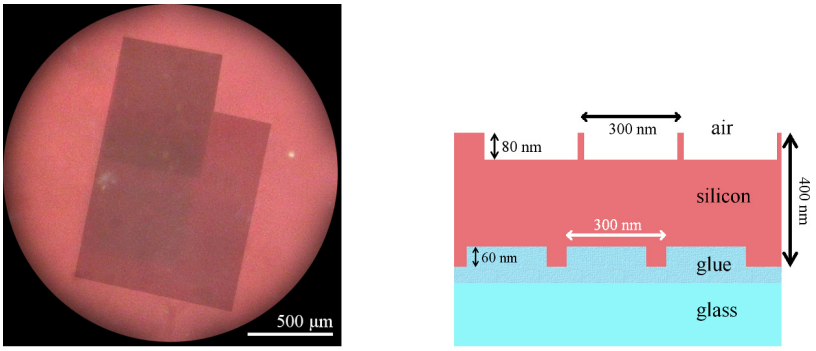

Fig. 2. (a) Microscope image (top view) of the fabricated 2D dual interface grating in a 400 nm thick a-Si:H slab on glass. The top and bottom grating are independently patterned by e-beam lithography. The two gratings can be clearly identified, as they have been off-set to facilitate individual characterisation. (b) Cross-sectional scheme of the fabricated structure.

3. Measurements and results

The absorption of the structured film is characterized with a white light laser source (NKT Photonics model SuperK^{TM} Compact) and an integrating sphere. The beam is linearly polarized and enters the sphere at an angle of three degrees to avoid reflectance losses. The reflected and transmitted signals are collected with a standard spectrum analyzer (Ocean Optics model USB 2000 +) at the top of the sphere. The total absorption is therefore given by $A = 1 – (T + R)$.

To verify its optical properties, we first measure the unpatterned a-Si:H film on glass and compare the resulting spectrum to a numerical simulation based on the scattering-matrix method [25], using dielectric functions derived from ellipsometry, see Appendix. Figure 3 shows very good agreement between the two spectra. Since NOA61 has the same refractive index as the glass substrate, the glue layer is considered as glass in the numerical calculations. Measured and calculated absorption spectra of the bottom, top and double-sided gratings are then plotted in Fig. 4. Again, we observe very good agreement in all three cases. We also note that the double-sided spectrum combines features of both individual gratings. Table 1 finally summarizes the measured integrated absorption as well as the absorption enhancement obtained by the different structures.

4. Discussion

Both the individual gratings show absorption enhancements compared to an unpatterned film. This is expected and well documented [26]. We are, however, not aware of comparable structures in the literature that do not use a metal back reflector (BR) or an anti-reflection coating (ARC). Our theoretical analysis therefore shows the potential of the dual interface grating approach, which leads to an absorption enhancement comparable to that of an unpatterned layer with ARC and metal (Ag or Al) back reflector (see Table 1). Higher enhancements may well be possible with further optimization.

Comparing the top and bottom gratings, we note that the top grating outperforms the bottom grating (32% vs 25%), which we attribute to antireflection action at the top grating. On the other hand, the bottom grating only diffracts light that has already experienced a single pass and therefore tends to act mostly in the long wavelength range, as most of the short-wavelength light has already been absorbed before it reaches the bottom grating.

#184707 - $15.00 USD Received 5 Feb 2013; revised 8 Mar 2013; accepted 11 Mar 2013; published 22 Apr 2013

Overall, the improvement of the dual grating is clearly apparent, but relatively modest. We believe that further optimization of the individual gratings and their combination will improve the performance; furthermore, an indirect bandgap material such as polycrystalline silicon will benefit more from our approach, as the propagation length is longer; in contrast, in a:Si, a significant fraction of the incoming light is already absorbed in a single pass.

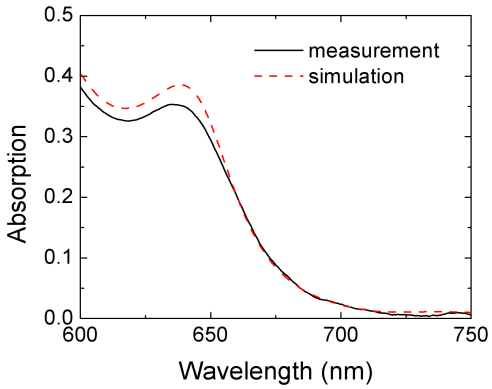

Fig. 3. Measured absorption characteristics of the unpatterned a-Si:H film deposited by plasma enhanced chemical vapor deposition (PECVD). The 400 nm thin film is characterised with a white light laser source and an integrating sphere.

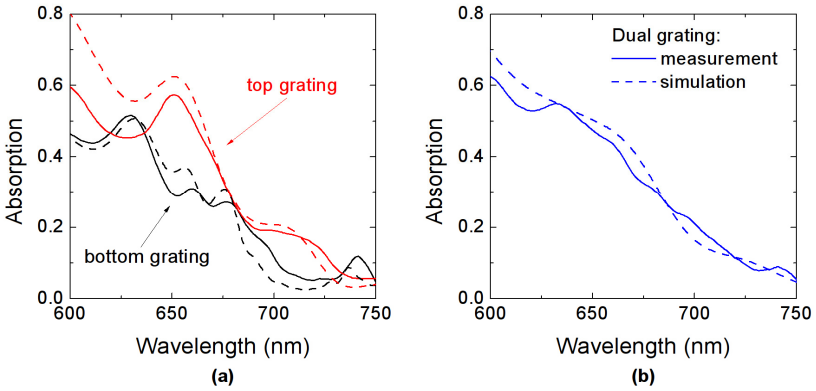

Fig. 4. Measured absorption characteristics of the patterned a-Si:H film. The measurements are taken with a white light laser source and an integrating sphere (solid line) and afterwards compared to numerical results (dashed line). (a) The measured spectrum for Fig. 1(a) is in excellent agreement with the simulated spectrum, while for the top grating of Fig. 1(b) we observe disagreement in the short-wavelength range. We think this discrepancy is due to the lattice structure used in the simulations, since the top grating is not perfectly described by either a lattice of circular holes or a chessboard lattice. (b) The dual grating shows a very good level of agreement between measured and simulated spectrum.

Table 1. Measured absorption and absorption enhancement of a 400 nm thick a-Si:H slab on glass following e-beam patterning. The measurements were integrated over the wavelength range from 600 nm to 750 nm. For comparison the calculated results of a structure consisting of a Ag/Al BR, the a-Si:H slab and a 70 nm Si_3N_4 ARC are also included (last column). The calculated absorption of the unpatterned film without BR and ARC is 16% instead of the measured 15%, which explains the lower enhancement of the simulated structure.

	unpatterned	bottom	top	bottom + top	unpatterned-ARC-(Ag/Al)*
absorption	15%	25%	32%	33%	34% / 32%
enhancement	0%	65%	110%	115%	110% / 93%

*unpatterned film with ARC and silver or aluminum BR (simulated structure for comparison)

#184707 - $15.00 USD Received 5 Feb 2013; revised 8 Mar 2013; accepted 11 Mar 2013; published 22 Apr 2013

5. Summary

We demonstrate a simple layer transfer technique using Norland Optical Adhesive 61 and show how a 400 nm thin film of hydrogenated amorphous silicon (a-Si:H) on glass can be patterned from both sides independently. The absorption characteristic of the dual grating structure is measured and is in very good agreement with numerical calculations. The dual grating structure shows an appreciable improvement over single gratings patterned either on the top or bottom of the film, which highlights the promise of the approach; further improvements are clearly possible by optimizing the parameters of both gratings independently, and/or by incorporating a metal mirror as the last step of the fabrication procedure. The layer transfer technique we demonstrate opens a new way to study dual interface gratings without any restriction on the design parameters.

Appendix

Spectroscopic ellipsometry (SE) measurements are performed with a variable angle spectroscopic ellipsometer (VASE®) from J. A. Woollam Co., Inc. in the 0.3 – 2.5 μm wavelength range with a 10 nm-step and angles of incidence of 65°, 70° and 75°. SE data are analyzed using WVASE32® dedicated software which adopts a multilayer model for the samples: this includes the glass substrate dielectric functions (as derived on a reference sample) and the a-Si:H thin film, whose dielectric function and thickness were free-parameters of the best-fit procedure. In particular, the a-Si:H dielectric functions at the absorption edge have been modelled with a Tauc-Lorentz oscillator model. The results for the complex dielectric function are shown in Fig. 5. The imaginary part has the typical form for a-Si:H with a direct energy gap around 730 nm (1.7 eV). The results for both real and imaginary parts of the dielectric function are in good agreement with literature, see e.g. [27].

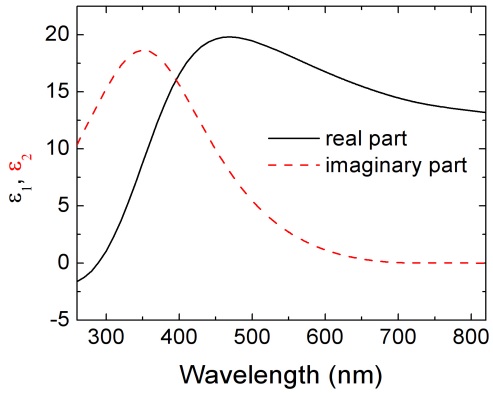

Fig. 5. Real and imaginary parts of the dielectric function of the a-Si:H layer determined by spectroscopic ellipsometry.

Acknowledgments

We like to acknowledge Steven Balfour and Callum Smith for helpful technical support. This work was supported by the EU through Marie Curie Action FP7-PEOPLE-2010-ITN Project No. 264687 “PROPHET”.